

Low-temperature CO oxidation over manganese, cobalt, and nickel doped CeO₂ nanorods

Deshetti Jampaiah,^a P. Venkataswamy,^b Victoria Elizabeth Coyle,^a Benjaram M. Reddy*^b and Suresh K. Bhargava*^a

^aCentre for Advanced Materials & Industrial Chemistry (CAMIC), School of Applied Sciences, RMIT University, GPO BOX 2476, Melbourne–3001, Australia

^bInorganic and Physical Chemistry Division, Indian Institute of Chemical Technology (IICT), Hyderabad - 500 007, Uppal Road, India

Corresponding authors*

E-mail: bmreddy@iiict.res.in; Tel: +91 40 27193510

E-mail: suresh.bhargava@rmit.edu.in; Tel: +61 3 9925 3365

Table S1 The Mn, Co, and Ni content of $\text{Ce}_{0.9}\text{Mn}_{0.1}\text{O}_{2-\delta}$ (Mn-CeO₂), $\text{Ce}_{0.9}\text{Co}_{0.1}\text{O}_{2-\delta}$ (Co-CeO₂), and $\text{Ce}_{0.9}\text{Ni}_{0.1}\text{O}_{2-\delta}$ (Ni-CeO₂) NRs determined from ICP-OES analysis.

Sample	Nominal metal content (%)	Calculated metal content (%)
Mn-CeO ₂	10	9.82
Co-CeO ₂	10	9.79
Ni-CeO ₂	10	9.87

Table S2 The T_{50} values of $\text{Ce}_{0.9}\text{Co}_{0.1}\text{O}_{2-\delta}$ (Co-CeO₂), and $\text{Ce}_{0.9}\text{Zr}_{0.1}\text{O}_{2-\delta}$ (Zr-CeO₂) NRs.

Sample	T_{50}	Reference
Zr-CeO ₂	265 °C	9
Co-CeO ₂	145 °C	Current work

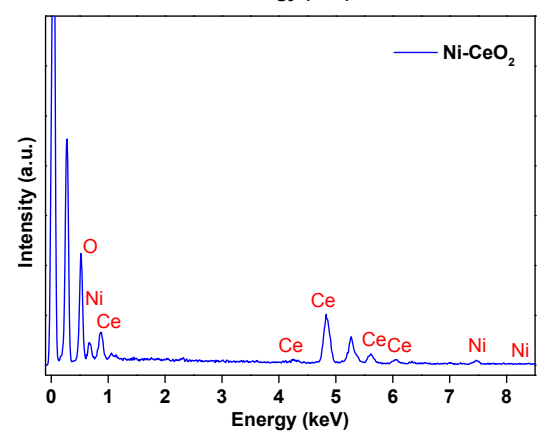
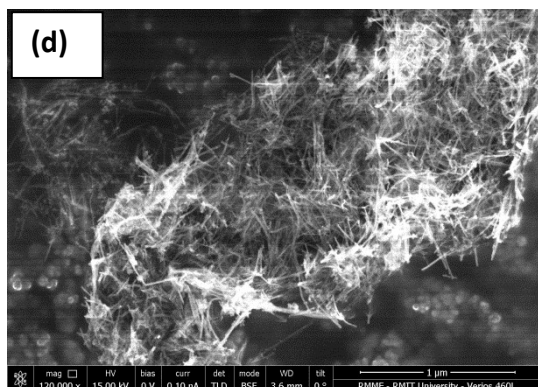
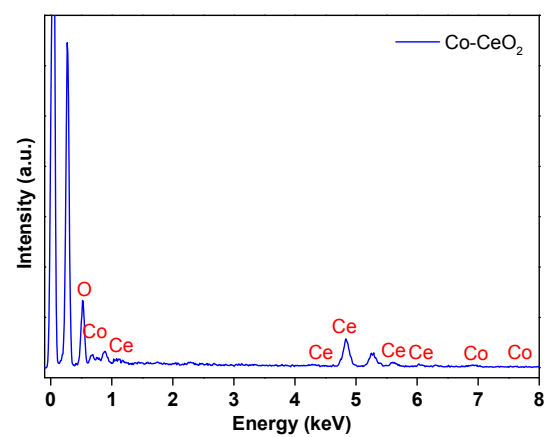
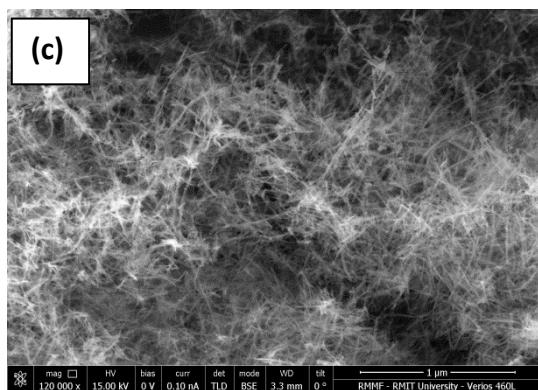
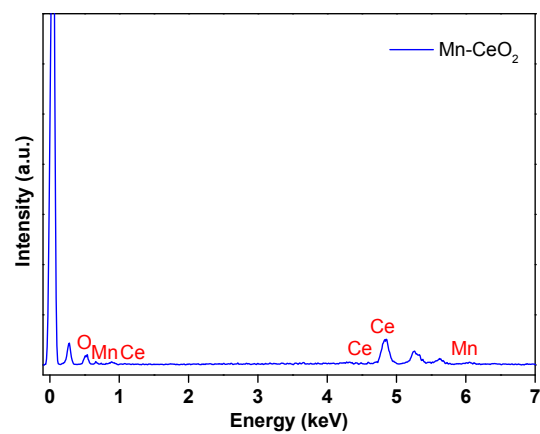
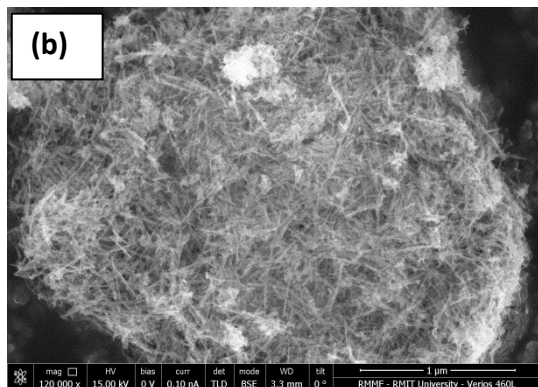
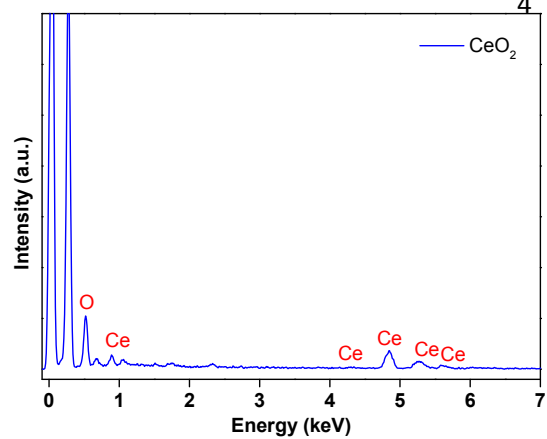
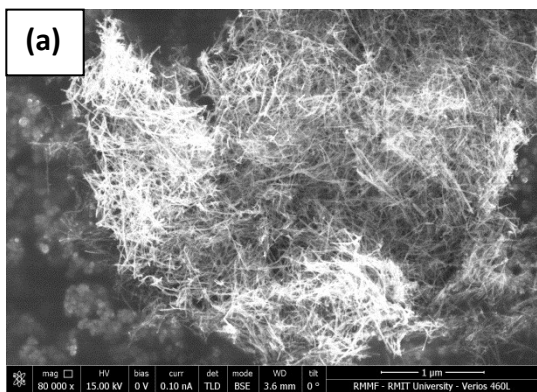


Fig. S1 SEM images of (a) CeO_2 , (b) $\text{Ce}_{0.9}\text{Mn}_{0.1}\text{O}_{2-\delta}$ (Mn- CeO_2), (c) $\text{Ce}_{0.9}\text{Co}_{0.1}\text{O}_{2-\delta}$ (Co- CeO_2), and (d) $\text{Ce}_{0.9}\text{Ni}_{0.1}\text{O}_{2-\delta}$ (Ni- CeO_2). The corresponding EDX spectra of the NRs.

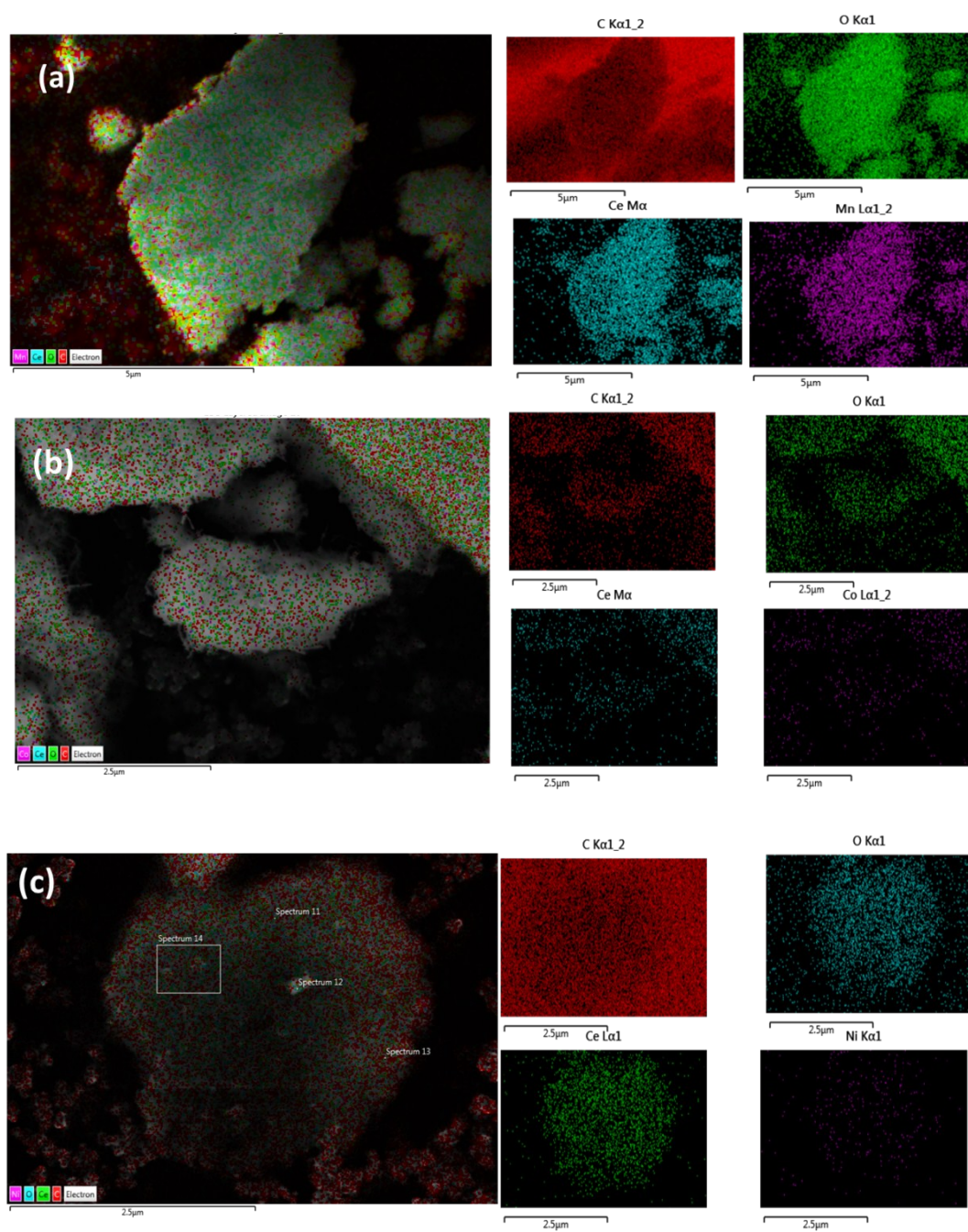


Fig. S2 EDX elemental mapping of (a) $\text{Ce}_{0.9}\text{Mn}_{0.1}\text{O}_{2-\delta}$ (Mn-CeO₂), (b) $\text{Ce}_{0.9}\text{Co}_{0.1}\text{O}_{2-\delta}$ (Co-CeO₂), and (c) $\text{Ce}_{0.9}\text{Ni}_{0.1}\text{O}_{2-\delta}$ (Ni-CeO₂) NRs.

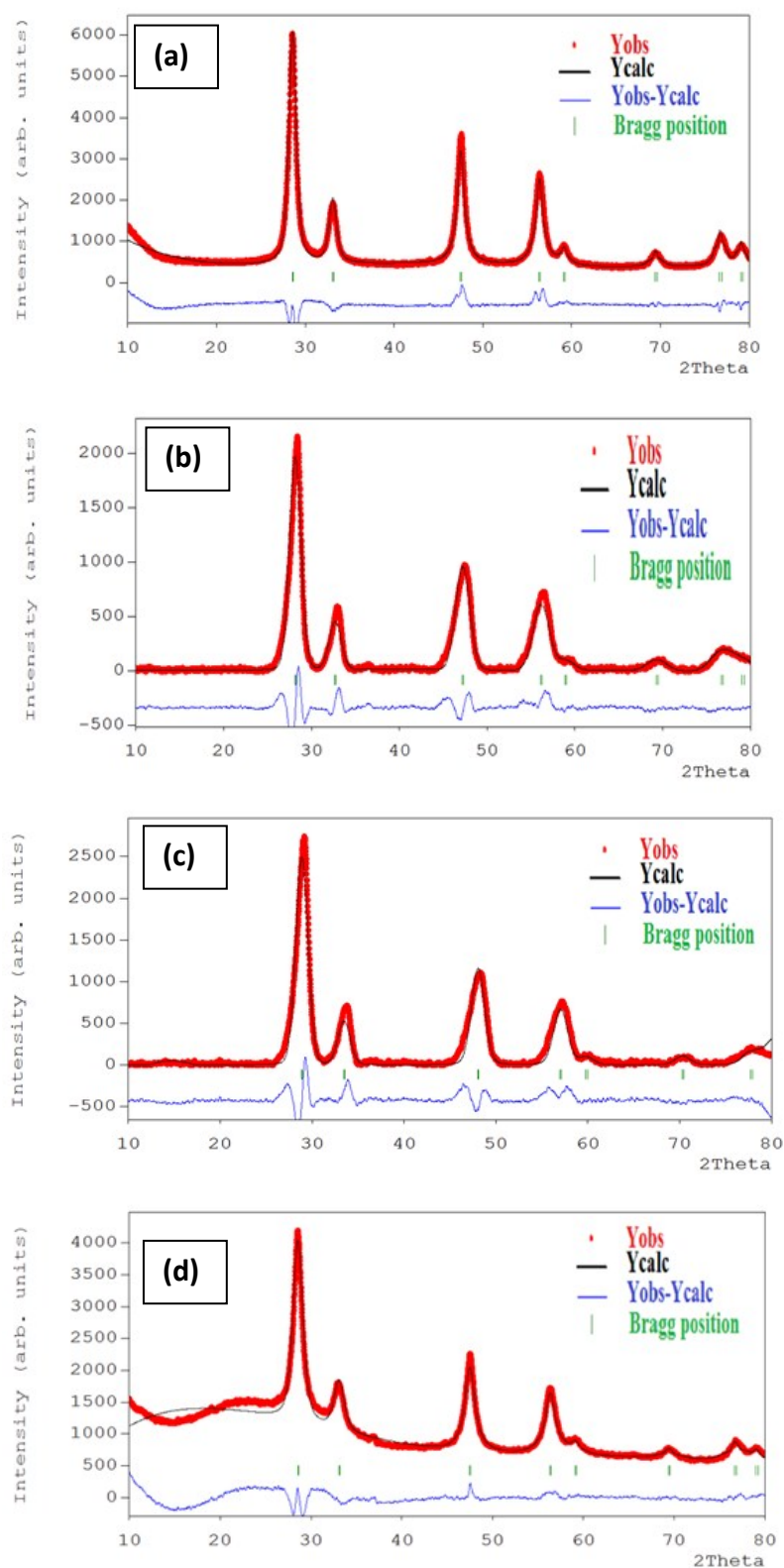


Fig. S3. Rietveld refinement of the XRD patterns of (a) CeO_2 , (b) $\text{Ce}_{0.9}\text{Mn}_{0.1}\text{O}_{2-\delta}$ (Mn- CeO_2), (c) $\text{Ce}_{0.9}\text{Co}_{0.1}\text{O}_{2-\delta}$ (Co- CeO_2), and (d) $\text{Ce}_{0.9}\text{Ni}_{0.1}\text{O}_{2-\delta}$ (Ni- CeO_2). Experimental data are indicated by red circles while the refined values form the continuous black line. The difference between the experimental and calculated curves is represented by the lowest blue line.

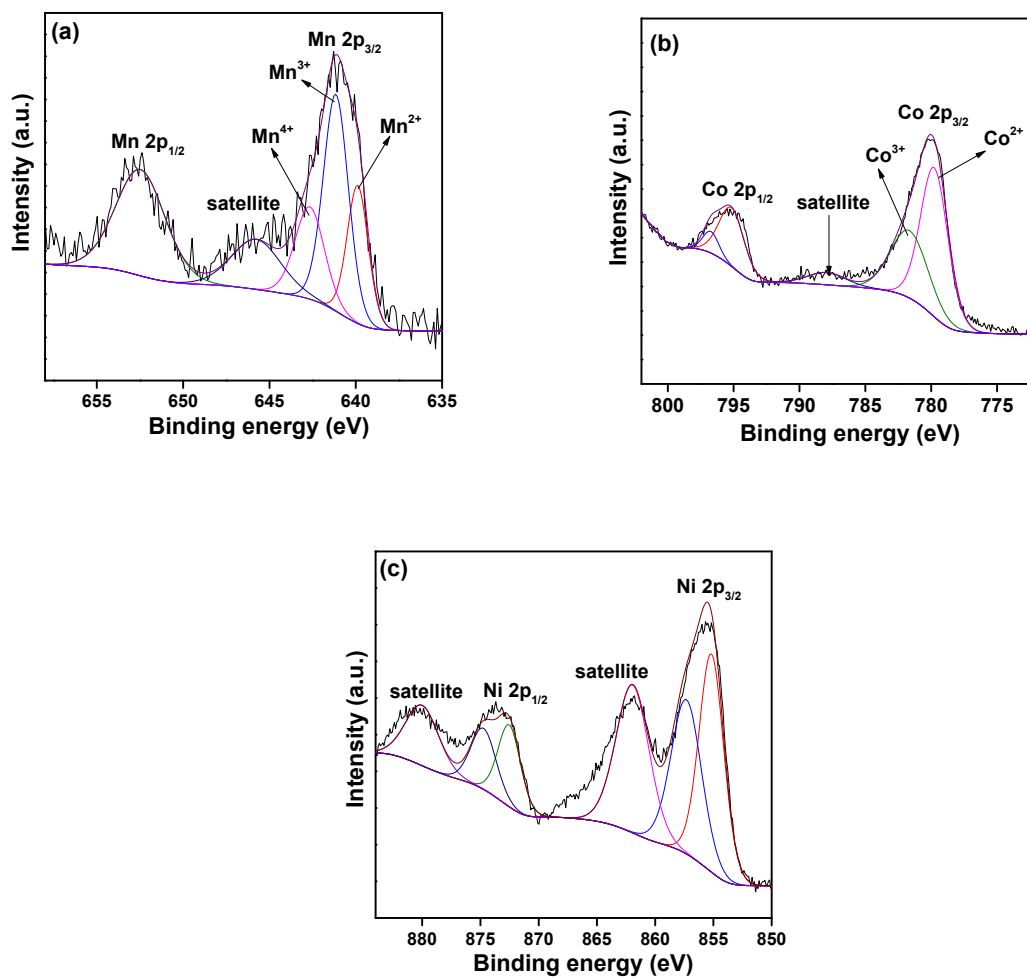


Fig. S4 XPS spectra of Ce_{0.9}Mn_{0.1}O_{2- δ} (Mn-CeO₂), Ce_{0.9}Co_{0.1}O_{2- δ} (Co-CeO₂), and Ce_{0.9}Ni_{0.1}O_{2- δ} (Ni-CeO₂) NRs; (a) Mn 2p, (b) Co 2p, and (c) Ni 2p.

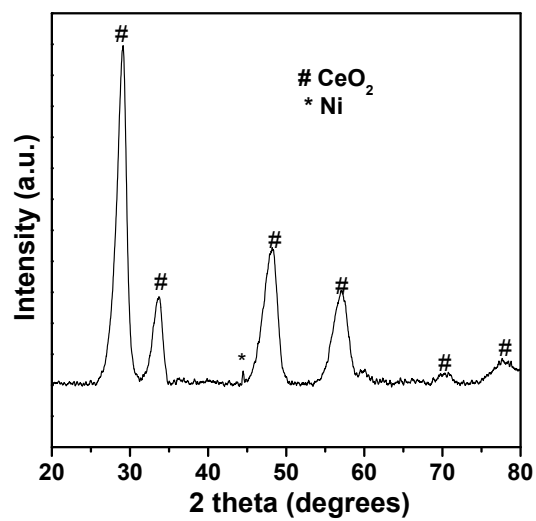


Fig. S5 XRD spectra of used $\text{Ce}_{0.9}\text{Ni}_{0.1}\text{O}_{2-\delta}$ (Ni- CeO_2) NRs

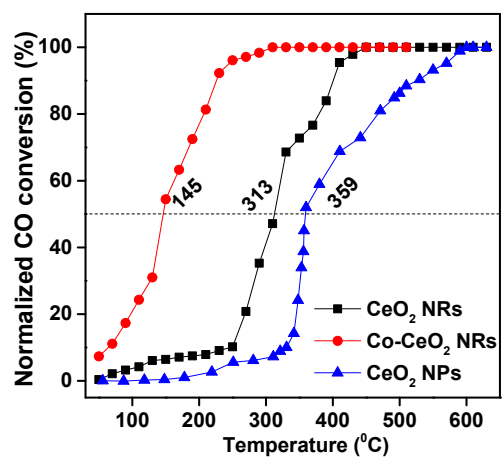


Fig. S6 Normalized CO conversions of CeO₂ NRs, Co-CeO₂ NRs, and CeO₂ NPs.

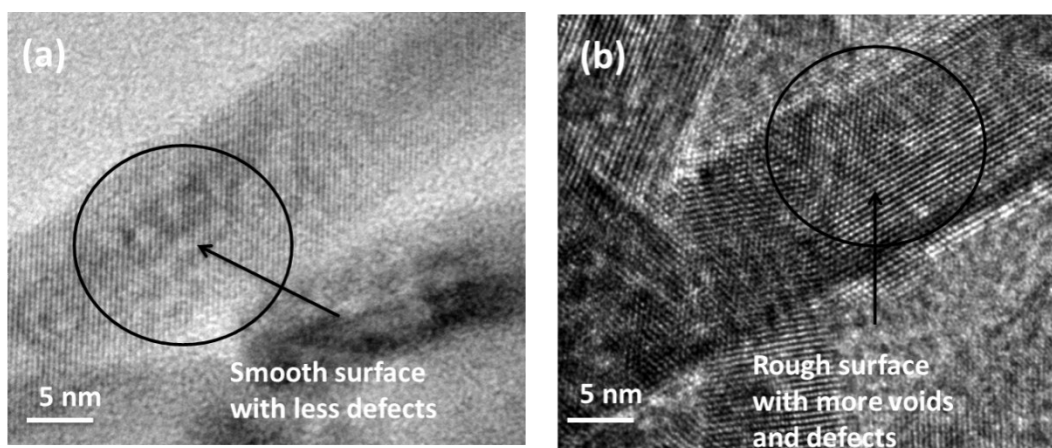


Fig. S7 HR-TEM images of (a) pure CeO_2 and (b) Co-CeO_2 NRs.